Appropriate Simplifications in Calculation of Mass Transfer in a Multicomponent Rate-Based Distillation Tray Model

2 **AUTHORS**, INCLUDING:

Ville Alopaeus
Aalto University

146 PUBLICATIONS **907** CITATIONS

SEE PROFILE

Appropriate Simplifications in Calculation of Mass Transfer in a Multicomponent Rate-Based Distillation Tray Model

Ville Alopaeus* and Juhani Aittamaa

Department of Chemical Technology, Helsinki University of Technology, Helsinki, Finland

The Maxwell−Stefan approach has been successfully used to model mass transfer in distillation columns and other multicomponent separation processes. This approach leads to rather complicated and computationally intensive matrix calculations. In this work, several simplifications for a rate-based distillation tray model incorporating Maxwell−Stefan-type mass transfer are evaluated according to their accuracy in predicting tray performance. The tray model is based on an assumption of vapor flowing as a plug through a completely mixed liquid. Mass and heat transfer resistance on both sides of the interface is considered. The basic plug flow model, in which the number of mass transfer units in vapor phase is used to model the composition profiles in the vapor, proved to be quite accurate. In that model, constant effective interfacial compositions are assumed. These compositions are iterated during the solution of the model. Approximating the high-flux correction can ease the computational procedure without significant loss of accuracy. The use of overall mass transfer coefficients and the assumption of a single-phase resistance proved to be inadequate.

Introduction

The Maxwell−Stefan approach to mass transfer has been adopted by many researchers in the past two decades, with very promising results. However, these equations still seems to remain somehow obscure to a large number of scientists and engineers who are dealing with mass transfer models in their work. The best way to implement Maxwell−Stefan mass transfer models into reactor or mass transfer device models is not clear, and various calculational approaches are adopted without consideration of their validity, at least quantitatively.

New approximations for these quite complex equations have been presented recently. In this article, some aspects regarding practical application of these equations and their effects on simulation results are studied. Various (simplified) formulations are tested with a plug flow plate model, which is in a central position in the chemical engineering practice.

The starting point here is the Maxwell−Stefan diffusion equations with Toor−Stewart−Prober linearization of constant physical properties in the diffusion path. This assumption is validated in many instances, and hence, a more complicated numerical integration over the mass transfer film thickness is not needed. Then, interphase mass and heat transfer is calculated by assuming resistance in both phases. Mass transfer coefficients are calculated from some suitable correlation.[1]

The equation for the mass transfer fluxes is written in the following form (reaction effects in the mass transfer region are neglected)

$$(N) = (J) + N_t(x) = c_t[k^\bullet](x_I - x_B) + (x_I)N_t \quad (1)$$

For the other phase, subscripts I (interface) and B (bulk

liquid or vapor) are interchanged so that the mass transfer direction is the same for both phases.[2,3]

The computational sequence for mass transfer calculations is the following:

1. Obtain all of the needed physical properties from the thermodynamic models, such as binary diffusion coefficients, densities, and viscosities of the two phases. Also obtain other system properties needed in mass transfer coefficient correlations. These are, for example, terminal velocity and drop or bubble size for vapor−liquid or liquid−liquid systems.

Binary diffusion coefficients at infinite dilution are usually obtained from correlations. For gases and lean liquid mixtures, these values may be satisfactory, but for concentrated liquids, they may differ from the observed values. There are a few methods for making a correction in the concentrated liquids. The following form has been suggested for taking the high mole fraction correction into account.[3]

$$Đ_{ij} = (Đ_{ij}^0)^{(1+x_j-x_i)/2}(Đ_{ji}^2)^{(1+x_i-x_j)/2} \quad (2)$$

This form has been adopted here as a basis for diffusion coefficient calculations. This issue has been discussed in more detail elsewhere.[4]

2. Calculate matrix of inverted diffusion coefficients and invert it to the (Maxwell−Stefan) diffusion coefficient matrix.[3]

3. From steps 1 and 2, calculate the Reynolds number and the matrix of Schmidt numbers. The multicomponent diffusion coefficient matrix is used in the Schmidt number instead of the scalar diffusion coefficient.

4. Calculate the matrix of mass transfer coefficients using some suitable correlations. These are often of type Sh = a + bRe^nSc^m. The multicomponent mass transfer coefficient matrix[5] is calculated then as

$$[k] = \frac{a}{d}[D] + \frac{bRe^n\mu^m}{d\rho^m}[D]^{1-m} \quad (3)$$

* Corresponding author. Present address: Neste Engineering Oy, P.O. Box 310, 06101 Porvoo, Finland. E-mail: Ville.Alopaeus@fortum.com. Fax: +358 10 45 27221.

If there is a single film thickness that can be explicitly known, the mass transfer coefficient matrix is obtained in a straightforward manner from the diffusion coefficient matrix as

$$[k] = 1/l[D] \qquad (4)$$

This is equivalent to eq 3 with $b = 0$ and $a = d/l$. It should be noted that, in that case, no matrix fractional power is needed.

Next, calculate the mass transfer rate factor matrix and then the high-flux correction matrix according to the chosen mass transfer model, e.g., the film or the penetration model. The high-flux correction takes account of the fact that the mole fraction profiles are not linear along the diffusion path.[3,6]

The total (convective) flux across the interface needed in these equations is obtained from the summation equation for the interface, that is, interface mole fractions are iterated until the mass transfer fluxes are equal at both sides of the interface and the sum of interface mole fractions is unity. If the mass transfer calculations are done in the same iteration loop with the distillation column or reactor model calculations, the total flux can usually be obtained from the material balances. Some examples are:

For a distillation tray

$$N_t = \frac{V_{j-1} - V_j + f_v F_j}{A} \qquad (5)$$

For a CSTR

$$N_t = \frac{\sum_{i=1}^{n} (F_v - P_v + V_v r_v)_i}{a_{mtr} V_R} \qquad (6)$$

For a single spherical particle, with reaction occurring inside, assuming pseudo-steady-state

$$N_t = \frac{d}{6} \sum_{i=1}^{n} r_i \qquad (7)$$

Sometimes, a relation between the diffusion and the mass transfer fluxes (the so-called bootstrap condition) can be found. Mass transfer fluxes can then be obtained explicitly from the diffusion fluxes and this relation alone, without iteration. The exact bootstrap condition can be found quite rarely. However, approximate relations are often available, as it is in distillation.

The bootstrap solution states that the mass transfer fluxes are not linearly independent, and thus a determinacy relation can be found. For distillation and other vapor–liquid mass transfer situations, such a relation can be found by assuming that the difference in conductive heat transfer fluxes between the two sides of the interface is negligible compared to the heats of vaporization. The energy balance for the interface then gives us the relation

$$\sum_{i=1}^{n} N_i H_{v,i} = 0 \qquad (8)$$

Then, the mass transfer fluxes can be calculated explicitly with the bootstrap matrix and the total flux from the sum of the component mass transfer fluxes.[3]

Another correction sometimes made in the mass transfer expression in eq 1 originates from the fact that the true driving force for diffusion is not the mole fraction gradient, but the gradient of chemical potential. This correction can be made by further multiplying the high-flux-corrected mass transfer flux equation by a matrix of thermodynamic corrections. For nonideal gas mixtures, the corresponding correction can be made as well. This is, however, necessary only in very high pressures.[3]

The use of a thermodynamic correction with the empirical mass transfer coefficient correlations is not an obvious question. When the mass transfer coefficient correlations are obtained from measurements of thermodynamically ideal systems and these correlations are to be used in nonideal systems, then the use of a thermodynamic correction factor is justified. However, if the correlations are obtained from measurements of nonideal systems, the introduction of a thermodynamic correction afterward may lead to errors. One more complication is that the thermodynamic correction strongly depends on the chosen thermodynamic model. Consequently, an accurate activity coefficient model must be used. The activity coefficient model should predict both the activity coefficients and their derivatives with respect to mole fractions accurately.

Some Calculation Methods for the Interphase Mass Transfer

To calculate interphase mass transfer, single-component mass transfer fluxes must be calculated at both sides of the interface. The interface compositions and the total flux are then iterated so that the mass transfer fluxes are equal and the mole fractions at both sides of the interface sum to unity. This procedure can be done separately in an inner loop of some separation unit or reactor model solution or, preferably, simultaneously with the other model equations.

Often, it is desirable to remove the interface compositions in the mass transfer equations. In these cases, the two mass transfer resistances are usually combined to an overall mass transfer coefficient. The set of equations is then diminished for faster solution. On the other hand, composition profiles can be pre-integrated in the plug flow type configurations, leading to a simpler formulation of the model equations. The overall mass transfer coefficient matrix for multicomponent systems is usually defined by a straight generalization of the corresponding binary form, leading to

$$[k_{OV}^\bullet]^{-1} = [k_V^\bullet]^{-1} + \frac{c_t^V}{c_t^L}[M][k_L^\bullet]^{-1} \qquad (9)$$

Here, $[M]$ is the phase equilibrium linearization matrix, $M_{ij} = \partial y_i^*/\partial x_j$. If the distribution coefficients can be described by the form $K_i = p_i^S \gamma_i/p$, then this matrix is equal to $[K][\Gamma]$, where $[K]$ is a diagonal matrix of $n - 1$ first distribution coefficients

The equation for overall coefficients can be derived for binary systems by assuming negligible total flux (even though the high-flux correction to the mass transfer coefficients is shown here). For multicomponent systems, the derivation is not possible, as vectors cannot be subtracted from the matrix equations. This is why the equation for overall mass transfer coefficients must be defined by the above equation.[3,7]

If the mass transfer coefficient matrices are calculated using bulk compositions (and temperatures), instead of film averages, the interphase mass transfer can be calculated by iterating total flux only. This is accomplished by the following procedure. First, interface compositions are calculated by equating the flux values for the both sides of the interface as

$$(x_\mathrm{I}) = \{c_\mathrm{t}^\mathrm{L}[k_\mathrm{L}^\bullet] + N_\mathrm{t}[I] + c_\mathrm{t}^\mathrm{V}[k_\mathrm{V}^\bullet][K]\}^{-1} \{c_\mathrm{t}^\mathrm{V}[k_\mathrm{V}^\bullet](y_\mathrm{B}) + N_\mathrm{t}(y_\mathrm{B}) + c_\mathrm{t}^\mathrm{L}[k_\mathrm{L}^\bullet](x_\mathrm{B})\} \quad (10)$$

The total flux must be known when the above equation is used. The residual of the summation equation (for iterating the total flux) for an equation solver is then obtained from

$$F = \sum_{i=1}^{n-1} K_i x_{\mathrm{I},i} + K_{nc}\left(1 - \sum_{i=1}^{n-1} x_{\mathrm{I},i}\right) - 1 \quad (11)$$

The mass transfer fluxes are then calculated from eq 1, as the convective part (the total flux) is known.

Computational Simplifications

Some steps in the calculation of the mass transfer fluxes can be simplified to ease the computational burden. First, in eq 3 for multicomponent systems, a fractional power for a matrix is needed. This can be achieved approximately, by using binary mass transfer coefficients[3] or by using the knowledge of the structure of the diffusion coefficient matrix. Matrix fractional powers can be calculated approximately for matrices with diagonal elements relatively greater than their off-diagonal elements.

For a problem $[A] = [D]^p$, we have the following approximate formulas

$$A_{ii} = D_{ii}^P \quad \text{for diagonal elements} \quad (12)$$

$$A_{ij} = D_{ij}\frac{D_{ii}^P - D_{jj}^P}{D_{ii} - D_{jj}} \quad \text{for off-diagonal elements} \quad (13)$$

Other matrix functions can be approximated similarly. For $[A] = f([D])$, we can use the following[8]

$$A_{ii} = f(D_{ii}) \quad \text{for diagonal elements} \quad (14)$$

$$A_{ij} = D_{ij}\frac{f(D_{ii}) - f(D_{jj})}{D_{ii} - D_{jj}} \quad \text{for off-diagonal elements} \quad (15)$$

Another simplification can be made for the high-flux corrections. After linearization, the following approximate formulas give quite satisfactory results in most of the mass transfer calculations. The high-flux-corrected mass transfer coefficient matrix is given simply by[9]

$$[k_\mathrm{I}^\bullet] = [k_\mathrm{I}] - aN_t/c_\mathrm{t}[I] \quad (16)$$

where the linearization parameter a can be calculated from the following equations: for the film theory

$$a = \frac{1}{\Psi_{\mathrm{ave}}} - \frac{1}{\exp(\Psi_{\mathrm{ave}}) - 1} \quad (17)$$

and for the penetration theory

$$a = \frac{1}{\Psi_{\mathrm{ave}}}\left[1 - \frac{\exp(\Psi_{\mathrm{ave}}^2/\pi)}{[1 + \mathrm{erf}(\Psi_{\mathrm{ave}}/\sqrt{\pi})]}\right] \quad (18)$$

Here

$$\Psi_{\mathrm{ave}} = N_\mathrm{t}(n - 1)/(c_\mathrm{t}\,\Sigma k_{ii}) \quad (19)$$

The Plug Flow Models

Basic Two-Film Model. Mass transfer calculations here are made using a plug flow model. This model is thought to be a good representative of a typical mass transfer situation, and furthermore, it has some features not found in simple two-film calculations, where both phases are assumed well mixed. Here, the vapor phase is assumed to flow as a plug through a well-mixed liquid, which is often a reasonable approximation to small distillation trays and to several other pieces of equipment appearing in the chemical industry. There is a resistance to mass and heat transfer in both phases (although in some cases resistance can be assumed to be in one phase only). [10]

The variables for the model are the following: average mole fractions in the V phase (n in number), average mole fractions at the interface (n), mole fractions at the L phase (n), distribution coefficients (n), molar fluxes (n), and temperatures of the interface, V phase, and L phase. This makes total $5n + 3$ variables. V refers here to the vapor phase and L to the liquid phase. The equations to be solved are the mass transfer flux equations for both films and an energy balance for both phases. Composition profiles for the dispersed phase must also be solved. The average compositions in the V phase are kept as variables, because these compositions are needed in the diffusion coefficient matrix in the V phase. Some variables can be left out of the previous list if the values calculated in the same iteration loop are used. For example, distribution coefficients can be calculated at the beginning of a loop, and these values can be used in the rest of that loop. The same is true for mass transfer fluxes, as these are needed only to check interface mole fractions and for the energy balance. However, for nonlinear systems, it is probably advisable to keep these variables in the set, as this is thought to make the system more linear (even though larger), which makes it easier, and sometimes even faster, to solve. Variables of the basic plug flow model are illustrated in Figure 1.

Pressure is assumed constant everywhere in the considered system. The interface is assumed to be in equilibrium, that is

$$y_{\mathrm{I},i} = K_i x_{\mathrm{I},i} \quad (20)$$

where

$$K_i = \gamma_i p_i^\mathrm{S}/p \quad (21)$$

The mass transfer coefficients are calculated from the diffusion coefficients and other required properties for both phases. The mass transfer fluxes are calculated as

$$(N_\mathrm{V}) = c_\mathrm{t}^\mathrm{V}[k_\mathrm{V}^\bullet](y_{\mathrm{B,ave}} - y_\mathrm{I}) + (y_{\mathrm{B,ave}})N_\mathrm{t} \quad (22)$$

$$(N_\mathrm{L}) = c_\mathrm{t}^\mathrm{L}[k_\mathrm{V}^\bullet](x_\mathrm{I} - x_\mathrm{B}) + (x_\mathrm{I})N_\mathrm{t} \quad (23)$$

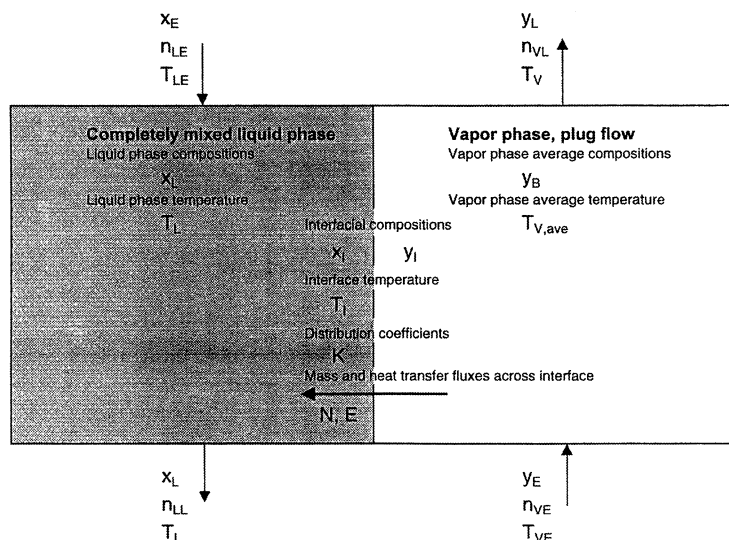In the previous equations, it is assumed that the fluxes

Figure 1. Illustration of the basic two-film plug flow model.

can be calculated with the average interfacial compositions. These averages are obtained from the solution of the flux equations along with the rest of the set of equations. The assumption that the average interfacial compositions can be used is verified later.

The number of mass transfer units for the V phase is calculated by assuming that the total vapor flow varies linearly over the height of the stage, which gives

$$[N_V] = c_t^V \frac{2A}{n_{VE} + n_{VL}} [k_V^\bullet] \qquad (24)$$

from which the average mole fractions in the V phase can be calculated as

$$(y_{B,ave}) = (y_I) - \{[I] - \exp(-[N_V])\}[N_V]^{-1}(y_I - y_E) \qquad (25)$$

and the mole fractions above the stage as

$$(y_L) = (y_I) - \exp(-[N_V])(y_I - y_E) \qquad (26)$$

The last mole fraction is then obtained from the relation[3] $\Sigma x = 1$.

The liquid-phase mole fractions are obtained from the material balance as

$$(x_B) = \frac{n_{LE}}{n_{LL}} (x_E) + \frac{A}{n_{LL}}(N) \qquad (27)$$

In fact, the mole fractions above the vapor phase are preferably calculated from the material balances as well, instead of eq 26. If the present tray model is to be used in a column model, it is very important for the column model convergence that the material balances of each tray be solved to high precision, and the matrix calculations of eq 26 do not necessarily do that. Hence, the mole fractions of the vapor leaving the stage are calculated from

$$(y_L) = \frac{n_{VE}}{n_{VL}}(y_E) - \frac{A}{n_{VL}}(N) \qquad (28)$$

The average temperature of the V phase is assumed to be the arithmetic average of the temperatures of the entering and leaving streams, i.e., $T_{V,ave} = (T_V + T_{VE})/2$. Additional heat can be supplied to the L phase. Energy balance (divided by the mass transfer area) then reads for the V phase

$$\frac{n_{VE}}{A}\sum_{i=1}^{n} y_{E,i} H_{VE,i} = h_V(T_{V,ave} - T_I) + \sum_{i=1}^{n} H_{VI,i} N_i + \frac{n_{VL}}{A}\sum_{i=1}^{n} y_{L,i} H_{VL,i} \qquad (29)$$

for the L phase

$$\frac{n_{LE}}{A}\sum_{i=1}^{n} x_{E,i} H_{LE,i} = h_L(T_I - T_L) + \sum_{i=1}^{n} H_{LI,i} N_i + \frac{Q}{A} = \frac{n_{LL}}{A}\sum_{i=1}^{n} x_{L,i} H_{LL,i} \qquad (30)$$

and for the interface

$$h_V(T_{V,ave} - T_I) + \sum_{i=1}^{n} H_{VI,i} N_i = h_L(T_I - T_L) + \sum_{i=1}^{n} H_{LI,i} N_i \qquad (31)$$

Molar flows out from the balance region (divided by the mass transfer area) can be calculated from

$$\frac{n_{VL}}{A} = \frac{n_{VE}}{A} - \sum_{i=1}^{n} N_i \qquad (32)$$

$$\frac{n_{LL}}{A} = \frac{n_{LE}}{A} + \sum_{i=1}^{n} N_i \qquad (33)$$

The liquid and vapor enthalpies are calculated by assuming constant heat capacity for each component.

$$H_{L,i} = c_{mL,i}(T - T^0) \tag{34}$$

$$H_{V,i} = H_{V,i}^0 + c_{mV,i}(T - T^0) \tag{35}$$

Solving the Equations. The residuals for an equation solver are obtained in the following manner The

Interface ($n - 1$ in number)

$$F_N = N_V - N_L \tag{36}$$

Flux equations ($n - 1$)

$$F_N = N_L - N_{solver} \tag{37}$$

Average mole fractions in the V phase (n)

$$F_V = y_{B,ave} - y_{B,ave,solver} \tag{38}$$

Average mole fractions in the L phase (n)

$$F_L = x_B - x_{B,solver} \tag{39}$$

Distribution coefficients (n)

$$F_K = K_i - K_{i,solver} \tag{40}$$

Summation equations for both sides of the interface

$$F_{Sx} = \Sigma x_I - 1 \tag{41}$$

$$F_{Sy} = \Sigma y_I - 1 \tag{42}$$

set of equations is completed by energy balance equations, one for each phase and one for the interface. This makes total $5n+ 3$ equations, and the set is closed. This set of equations can be solved by a standard algebraic equation solver, e.g., Newton−Raphson.

Differential Plug Flow Model. In the basic model, average interface compositions were used to calculate the mass transfer fluxes. This assumption is verified by dividing the vapor into slices and iterating the local interfacial compositions and temperature at each point. This allows true local vapor properties to be used in material balance equations and in energy balance equations as well.

In the differential plug flow model, the liquid-phase compositions and temperature are iterated by solving the average mass transfer and energy fluxes. This is done with two iteration loops. Variables in the outer loop are liquid-phase compositions (n in number), total flow out, and temperature. This makes total $n + 2$ variables. Liquid-phase mole fraction residuals are obtained by equating calculated and solver-given values. The liquid-phase mole fractions are calculated from eq 27, with average mass transfer fluxes. The residual for the liquid-phase energy balance is obtained from eq 30, again with averaged energy flux values. The residual for the total flow is obtained from eq 32, with average mass transfer fluxes.

The average flux values are obtained from the same model as is used in the basic plug flow model, except that the liquid-phase compositions and temperature are obtained from the outer iteration loop and the corresponding residual equations are neglected. The vapor side is divided into slices, and the fluxes for each of these slices are calculated in sequence, using the output
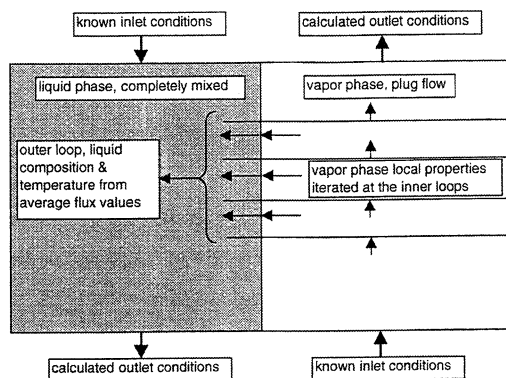

Figure 2. Schematic illustration of the differential plug flow model solution.

values from the previous slice as initial conditions. Then, the resulting fluxes are averaged for the outer loop. The calculation procedure is illustrated schematically in Figure 2.

The mass transfer area is assumed to be constant. This is to simplify the calculations, as the description of the flow conditions on a tray is considered a separate problem from the mass transfer calculations. This approach keeps the mass transfer calculations here more general, as the tray dimensions and hydraulic conditions need not be specified. In practice, these mass transfer calculations can then be combined with the flow description of a distillation tray.

In the solution of the differential flow model, it is very important that the inner loop be solved to high precision. If the precision in solution of the inner loop is not very high, then the outer loop is not converged. In practice, the inner loop tolerance should be at least the square of the outer loop tolerance. This is not a major problem, because as the system of nonlinear algebraic equations is close to solution, a Newton−Raphson-type equation solver converges rapidly and not many iteration steps are needed after a reasonably accurate solution is found.

Simulated System

A system of six light hydrocarbons is considered. The physical properties used in the present model are obtained by solving a standard distillation column model, implemented in a process flowsheet simulator. Then, the conditions of a suitable plate are chosen for the present model evaluation. This is to ensure that the properties are reasonable and physically possible. The simulated column had 45 plates, with feed to plate number 26 (from the bottom). Properties from plate 27 (one above the feed) were chosen for this study.

Vapor pressures are estimated[11] at the interface temperature. Diffusion coefficients are estimated with the Wilke−Chang correlation. The vapor phase is assumed to be an ideal gas, and the liquid phase is assumed to be thermodynamically ideal (i.e., all activity coefficients are assumed to be unity). Component mole fractions in the V and L phase feeds, and other physical properties (that are assumed constant), are shown in Tables 1−3. The reference temperature is taken to be 300 K.

Table 1. Components, Mole Fractions, and Physical Properties

component	x_V	x_L	V_m (m³/mol)	$H_{V,i}^0$ (J/mol)	c_{mV} (J/K mol)	c_{mL} (J/K mol)
propane	0.33	0.11	8.4×10^{-5}	14 305.3	75.6	123.4
n-butane	0.23	0.22	1.0×10^{-4}	20 890.8	100.4	144.9
i-butane	0.22	0.15	1.0×10^{-4}	18 910.0	99.9	144.1
n-pentane	0.08	0.22	1.2×10^{-4}	26 560.5	122.9	171.4
i-pentane	0.10	0.22	1.2×10^{-4}	25 072.2	121.6	167.7
n-hexane	0.04	0.08	1.3×10^{-4}	31 800.6	146.3	200.3

Table 2. Binary Ideal Dilution Diffusion Coefficients on the Liquid Side (10^{-9} m²/s)

0	8.764	10.32	6.795	7.380	5.687
11.37	0	8.791	5.790	6.288	4.845
11.29	7.416	0	5.750	6.245	4.812
9.910	6.510	7.664	0	5.482	4.224
9.928	6.522	7.678	5.057	0	4.232
8.856	5.817	6.849	4.511	4.899	0

Table 3. Binary Diffusion Coefficients on the Vapor Side (10^{-6} m²/s)

0	1.024	1.031	0.8884	0.8950	0.7939
1.024	0	0.8499	0.7262	0.7317	0.6447
1.031	0.8499	0	0.7313	0.7368	0.6493
0.8884	0.7262	0.7313	0	0.6254	0.5482
0.8950	0.7317	0.7368	0.6254	0	0.5524
0.7939	0.6447	0.6493	0.5482	0.5524	0

Other parameters needed in the simulation are the following:

$$l_V = 10^{-4} \text{ m}$$

$$l_L = 10^{-5} \text{ m}$$

$$n_{VE}/A = n_{LE}/A = 2.0 \text{ mol/(m}^2 \text{ s)}$$

$$p = 6.1 \text{ bar}$$

so that a constant and known film thickness is assumed for both films. Heat transfer coefficients can be calculated by assuming the same film thickness for heat transfer as for the mass transfer. This gives

$$h = \lambda/l \tag{43}$$

or from the Chilton−Colburn analogy

$$h = k \left(\frac{c_t c_m \lambda^2}{D^2} \right)^{1/3} \tag{44}$$

For multicomponent systems, some average values (e.g., mole averages) must be used in the previous equation.

If we use somehow typical values $\lambda_V = 0.02$ W/mK, $\lambda_L = 0.12$ W/mK, $D_V = 0.7 \times 10^{-6}$ m²/s, $D_L = 6 \times 10^{-9}$ m²/s, $c_t^V = 220$ mol/m³, $c_t^L = 9\ 200$ mol/m³, $c_{mV} = 115$ J/(K mol), $c_{mL} = 170$ J/(K mol), $k_V = 0.007$ m/s, and $k_L = 0.6 \times 10^{-3}$ m/s, then we have, for equal film thicknesses

$$h_V = 200 \text{ W/(m}^2 \text{ K)} \text{ and } h_L = 12\ 000 \text{ W/(m}^2 \text{ K)}$$

and from the Chilton−Colburn analogy

$$h_V = 190 \text{ W/(m}^2 \text{ K)} \text{ and } h_L = 5\ 100 \text{ W/(m}^2 \text{ K)}$$

We shall use the latter in our simulations. The high-molar-flux correction to the heat transfer coefficients is neglected in this study.[3]

Several computational aspects are studied and validated according to their impact on the calculated flux values. Various simplifications are compared to the "best available" method, which is chosen to be the Maxwell−Stefan diffusion model with the linearized equation of continuity (the Toor−Stewart−Prober approach). In the base cases, the Vignes correction is used for high mole fractions in the liquid binary diffusion coefficients. The validity of assuming constant effective interfacial compositions (the basic plug flow model) is validated by comparing the results to the differential vapor model, as are the assumption of linear composition profiles and the assumption of completely mixed vapor phase. Results when overall coefficients are used along with the assumption of a single-phase resistance are compared to the differential plug flow model as well. This is because the assumption of constant interfacial compositions is not needed in these models. The rest of the computational practices are validated by comparing the results to the basic plug flow model, as it illustrates explicitly the effect of these simplifications.

The studied computational procedures are the following: (1) calculation of the tray performance with the basic plug flow model, i.e., assumption of constant interfacial compositions (this assumption is made also in the rest of the cases); (2) use of ideal dilution binary diffusion coefficients in the liquid side, instead of correcting them for high mole fractions; (3) linearization of the high-flux correction term; (4) approximate calculations of matrix functions (eqs 12−15); (5) use of bulk mole fractions in the calculations instead of the film averages (then, eq 11 can be used for flux iterations with one variable for simple two-film calculations, when the bulk compositions are known); (6) use of the overall mass transfer coefficients; (7) effect of neglecting mass transfer resistance in one of the phases, when the mass transfer coefficients are considerably higher in that phase; (8) assumption of linear composition profiles in the vapor phase and calculation of arithmetic averages from the entering and leaving compositions instead of eq 25; (9) use of outlet compositions as effective vapor phase compositions, i.e., assumption of completely mixed vapor phase; and (10) the practice of calculating the bootstrap condition from the heats of vaporization.

For systems with large thermodynamic nonidealities, additional questions concerning computational aspects arise. Thermodynamic nonidealities appear in the calculation of the mass transfer fluxes in two ways. First, activity coefficients appear in the phase equilibrium expression in eq 21, relating compositions on both sides of the interface. This is a standard method of proceeding for both rate-based and ideal stage models and need not be considered any further here. Second, the composition derivatives of the activity coefficients appear in the correction for driving forces. As stated earlier, the correction for thermodynamic nonidealities along with an empirical mass transfer coefficient correlation is not a straightforward issue. In this work, the effect of the thermodynamic correction is not studied.

Numerical Results

In the base case, heat input into or out from the plate (Q/A) is varied, and inlet temperatures are kept at constant values of 335.3 K for the liquid phase and 337.7 K for the vapor phase. This is the situation when external heating or cooling is supplied to the plate or when there is a reaction in the liquid phase with

noticeable heat of reaction. Reaction effects are obviously not considered in the material balances, as these particular components would not react by themselves in the liquid phase. The point here is to change the thermal conditions within a plate to alter the total flux and hence molar flows over the plate to see the high-flux effects in the calculations. The range of heat inputs was quite large, so that, in extreme cases, about 20% of one phase was transferred to the other phase.

Comparisons are made by iterating the whole system with the different calculation methods and then comparing the resulting fluxes to the base case values (the differential vapor model).

The one-phase resistance assumption is tested by reducing the thickness of one film (here the L-phase film) and comparing the resulting fluxes to the fluxes calculated by assuming single-phase resistance, that is

$$N_{V,approx} = c_t^{V}[k_V^{\bullet}](y_{B,ave} - y^*) + (y_{B,ave})N_t \quad (45)$$

where

$$(y^*) = [K](x_B)$$

In this case, the residuals of the interface composition equations for the equation solver are obtained from the difference of the interface and bulk liquid compositions, so that the interface compositions become equal to the bulk values. The same approach is used for the overall coefficients, but the overall mass transfer coefficient from eq 19 is used instead of the vapor-phase mass transfer coefficient.

A similar equation can be used for the liquid phase, but it is not needed here because only liquid-phase resistance is assumed to be negligible. This assumption is sometimes made in distillation. The heat transfer coefficient is kept constant in this study.

The percentage error in the fluxes is calculated by the following equation.

$$E = 100n\frac{\displaystyle\sum_{i=1}^{n}|N_{approx} - N_{exact}|}{\displaystyle\sum_{i=1}^{n}|N_{exact}|} \quad (46)$$

This equation is used instead of the simple sum of relative errors of the single fluxes to prevent a large error resulting from a nearly zero mass transfer flux of some single component. In most cases, the present error criterion gives numerical values for the flux errors that are similar to those obtained from the sum of relative errors.

Other possible error criterion is obviously obtained by comparing composition of the flows leaving the tray, as calculated by the different methods. This is, however, a very conservative criterion, as the compositions are dictated mainly by the vapor–liquid equilibrium, and not very large differences in the numerical values can be found. Hence, the errors in the fluxes are used to pronounce the errors in the mass transfer calculations.

(1) The Basic Plug Flow Model. First, the number of slices needed to represent the differential plug flow was estimated. This estimate was made by altering the number of slices and calculating the corresponding average mass transfer fluxes. It was found that about five slices was enough, and not much additional im-

provement resulted when the number of slices was increased. To ensure the accuracy of the solution, 10 slices were used in the rest of this work.

The basic plug flow model gave errors between 0.6 and 7.5% as the heat input was altered. The largest errors occurred in the cases when all of the fluxes were quite small, so that the denominator in the error equation was small. The errors depend quite strongly on the value of the inlet flow divided by the mass transfer area, i.e., n_{VF}/A. This alters the number of mass transfer units and correspondingly affects the plate efficiencies. Relative errors in the fluxes as functions of n/A are shown in Figures 5 and 6. The highest errors (with the lowest n/A) correspond to number of mass transfer units ranging from about four to five, which is quite exceptional for a distillation tray.

All of these errors were so small that the basic plug flow model can be recommended for practical use. The differential plug flow model was considerably more complicated to solve than the basic model because of the solution of large number of nested iteration loops.

(2) Ideal Dilution Binary Diffusion Coefficients. The use of ideal dilution binary diffusion coefficients on the liquid side, instead of correcting them for high mole fractions, resulted in errors of approximately 10% in magnitude. The binary diffusion coefficients are not too far from each other in the present system, the relative difference being approximately 2 at the largest on both vapor and liquid side. For a system with a wider scale of binary diffusion coefficients, this error is expected to be larger.

Because the correction for high mole fractions is quite easily done, it is recommended as a standard practice even in the cases where the correction may be reasoned to be of minor importance. Another aspect strongly favoring the use of this correction is that it makes the diffusion coefficient matrices independent of the component numbering. The numbering dependency is found when infinite-dilution binary diffusion coefficients are used. These coefficients do not necessarily form a symmetric matrix in liquid phases, and because the last row of the binary diffusion coefficient matrix is not used in the formulation of the Maxwell–Stefan diffusion matrix, a numbering dependency results.

(3) and (4) Computational Simplifications of the High-Flux Correction. The high-flux correction can be linearized, and eqs 16–19 are then used for the high-flux correction. The total flux is known from the previous iteration step, and at the converged value this equals to the fluxes calculated using this linearization.

The matrix function simplifications, eqs 12–15, can be used to correct the mass transfer coefficient matrices in the following manner

$$f_i = \frac{N_t}{c_t\left[\exp\left(\dfrac{N_t}{c_t k_{ii}}\right) - 1\right]}$$

$$k_{ii}^{\bullet} = f_i \qquad \text{for diagonal elements}$$

$$k_{ij}^{\bullet} = k_{ij}\frac{f_i - f_j}{k_{ii} - k_{jj}} \qquad \text{for off-diagonal elements} \quad (47)$$

In Figure 3, relative errors are shown for the two approximate solutions

As the simplifications are made to the high-flux correction, the errors are slightly larger when the total
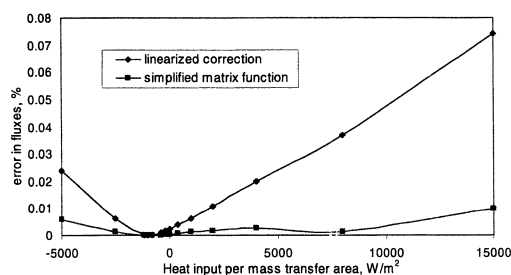
Figure 3. Relative errors for the linearized high-flux correction and for the high-flux correction matrix function simplification.
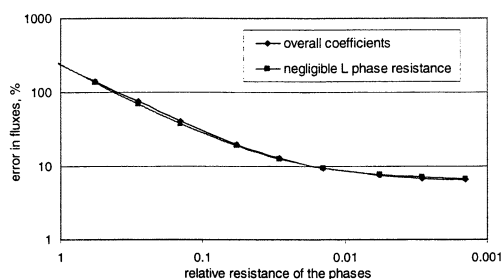

Figure 4. Relative errors in the fluxes for overall coefficients and for single-phase resistance as functions of relative resistance of the phases.

flux is larger. The errors were, however, so small in all cases that both of these methods can be well recommended. The matrix function simplification resulted in slightly lower errors than the high-flux correction simplification. However, it is slightly more dependent on the structure of the diffusion coefficient matrix, so that both methods can be ranked quite equally.

(5) Use of Bulk Compositions in the Diffusion Coefficient Matrices. This approach gave quite accurate results. The flux errors were, in all cases, less than 0.3%, which is a very good result indeed. On the other hand, as the interface compositions are iterated anyway, there is no reason to make this assumption in the full rate-based tray model.

The method of one-variable iteration was validated in a separate isothermal study. The results were good in terms of accuracy, but the iteration was slower than in the solution of the complete model. This is because of the extra matrix function calculation in eqs 10 and 11, and hence, the single-variable method is left only as an algebraic curiosity and is not recommended in practice.

(6) and (7) Overall Coefficients and Single-Phase Resistance. These two approximations were validated by altering the resistance in the liquid phase. The resulting errors are shown as a function of the relative resistance of the two phases.

$$R = \frac{c_t^V \sum\limits_{i=1}^{n-1} k_{V,ii}}{c_t^L \sum\limits_{i=1}^{n-1} k_{L,ii}} \tag{48}$$

In Figure 4, the relative errors in the fluxes are shown.

The errors are quite high for both methods, except when the resistance is very high for one phase only.
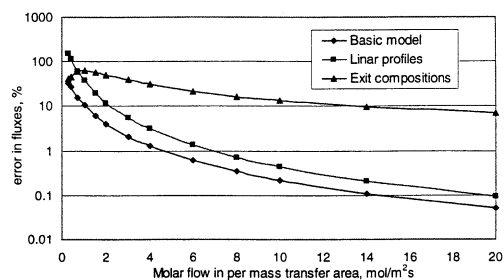

Figure 5. Errors in the basic plug flow model, errors as linear composition profiles are assumed, and errors as completely mixed vapor phase is assumed.

Even in the cases for which the liquid phase resistance is only one-tenth of the vapor phase resistance, the errors are approximately 25%. For equal resistance, the errors are approximately 250%.

Quite unexpected is that the overall coefficients resulted in larger errors in most cases compared to those found for the one-phase resistance assumption. An additional observation was that the overall coefficients resulted in a component numbering dependency. This is due to the use of only n − 1 distribution coefficients in the calculation of the overall mass transfer coefficients. It is suspected that the straightforward use of the distribution coefficients is not a correct method for combining the single-phase resistances.

Consequently, the use of overall mass transfer coefficients is not recommended. The assumption of a single-phase resistance is also quite doubtful, as it calls for a very large difference in the resistances to be reasonably accurate.

(8) and (9) Assumption of Linear Composition Profiles in the Vapor Phase and Assumption of Completely Mixed Vapor Phase. The assumption of linear profiles resulted in errors in fluxes of approximately 10% in the basic case, and the assumption of a completely mixed vapor phase resulted in approximately 50% errors. The errors depend significantly on the inlet flow rate divided by the mass transfer area. This value alters the number of mass transfer units. For systems with low numbers of mass transfer units, and correspondingly low efficiencies, the assumption of linear profiles was quite a good one. For systems with high numbers of mass transfer units, and correspondingly high efficiencies, the linearity assumption was quite poor. This is to be expected, as high-efficiency systems operate close to equilibrium for a large part of the flow. The assumption of a completely mixed vapor phase was poor in all cases. This is quite surprising, and it was expected that as high-efficiency systems (very low flow per mass transfer area) operate near equilibrium for a large part of the flow, the outlet compositions better represent the average behavior. Some indications of this behavior can be seen, but the errors were still quite large. The errors are shown in Figure 5.

Although this is clearly a noticeable error in the fluxes, the assumption of linear profiles eases the computational burden, as the calculation of the matrix exponential functions in eqs 25 and 26 are avoided. For high-efficiency systems, quite high errors are found for all cases. However, because the total operation of the plate depends both on the fluxes and on the mass transfer area, a more illustrative criterion for the mass transfer calculation accuracy is obtained if the errors
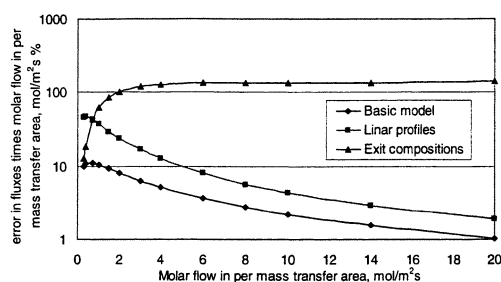
Figure 6. Flux errors in the three flow models multiplied by the inlet flow per mass transfer area.

in the fluxes are multiplied by the flow per mass transfer area. Then, high errors in fluxes, resulting from the low flux values, are multiplied by a high mass transfer area. These modified error values are shown in Figure 6.

From Figure 6, a clear trend can be seen. The assumption of linear profiles results in an error that is approximately three times larger than the error in the basic plug flow model. The assumption of a completely mixed vapor phase becomes worse and worse as the inlet flow per mass transfer area is increased.

In these comparisons, it was assumed that the flow in the actual plate is a complete plug flow. If the vapor is mixed, then the assumption of complete mixing is obviously better than shown here.

(10) Use of the Bootstrap Matrix. The use of the vaporization heat bootstrap matrix proved clearly inadequate in all cases. If the phase temperatures were very close to each other, the errors were a few tens of percents, but even a difference of 1 °C resulted in several hundred percent errors. Additionally, as the bootstrap solution does not ease the computation of a rate-based model to any degree, it is not recommended. Only if the use of the bootstrap condition leads to a completely explicit solution, it can be used with caution in some instances. In these cases, the high-flux correction should be made in the bootstrap matrix.[9]

Conclusions

A plug flow distillation tray model was used to compare certain simplifications quite often made in mass transfer calculations. The simultaneous mass and heat transfer, taking place on the modeled tray, was calculated with a two-film Maxwell–Stefan model. The following observations were made:

(1) The approximation of constant effective interfacial compositions over the froth height, along with the plug flow model, was quite satisfactory compared to a rigorous approach of dividing the vapor into differential slices. The assumption of linear composition profiles or a completely mixed vapor phase resulted in larger errors.

(2) The practice of calculating mass transfer fluxes using overall mass transfer coefficients leads to severe errors in the fluxes, except for a special case of truly equimolar transfer. The bootstrap solution using heats of vaporization also led to severe errors, except for the case where inlet and outlet temperatures of the phases were very close each other.

(3) Large errors were observed when the mass transfer resistance was assumed in one phase. Only if this assumption were justified by a very large difference in the mass transfer coefficients might it result in reasonably accurate fluxes. Even if the ratio of the mass transfer coefficients of the two phases were on the order of ten, there were still about 80% errors in the fluxes.

(4) The linearization of the high-flux correction (eq 16) and the approximate calculation of the matrix functions (eqs 14 and 15) resulted in negligible errors in all of the cases simulated here. Therefore, these simplifications can be used with confidence.

(5) The correction of binary liquid diffusion coefficients for high mole fractions seems to be reasonable but not compulsory, as the observed errors were not very large when this correction was omitted. This is partly due to some compensatory effect in these corrections. One aspect strongly favoring the use of the Vignes-type corrections for high mole fractions is that it makes the flux calculation independent of the component numbering by making the binary diffusion coefficient matrix symmetric.

(6) One-variable iteration for mass transfer fluxes was justified in terms of the approximation error. However, because the computational times were the same order of magnitude as, or even larger than, those in the corresponding exact solution, this method seems to be of no practical use.

Acknowledgment

Notation

General symbols

$[A]$ = a matrix (generally)

$[D]$ = matrix of Fick diffusion coefficients, as calculated from the Maxwell–Stefan equations (m²/s)

$[I]$ = identity matrix

(J) = diffusion flux (mol/m²s)

$[k]$ = mass transfer coefficient matrix (m/s)

$[k^\bullet]$ = high-flux mass transfer coefficient matrix (m/s)

$[M]$ = phase equilibrium linearization matrix

$[M']$ = mass transfer coefficient combination matrix

$[M'']$ = combination matrix for numbers of mass transfer units

(N) = mass transfer flux (mol/m²s)

ΔV = V phase change of molar flow rate

(x) = column matrix of component mole fractions

$[B]$ = matrix function of inverted binary diffusion coefficients (s/m²)

a = linearization parameter

A = mass transfer area (m²)

a, b = parameters

a_{mtr} = mass transfer specific area (m²/m³)

c_m = molar heat capacity (J/K mol)

c_t, c_t^V, c_t^L = total concentration and total concentration in V and L phases, respectively (mol/m³)

d = characteristic diameter (m)

D = diffusion coefficient (m²/s)

$\mathcal{D}_{ij}$ = binary diffusion coefficients (m²/s)

$\mathcal{D}_{ij}^0$ = binary ideal dilution diffusion coefficients (m²/s)

E = heat transfer flux (W/m²)

F = residuals for equation solver (various)

F_j = total feed rate to tray j (mol/s)

f_i = function in the calculation of approximate high-flux-corrected mass transfer coefficient (m/s)

f_V = vapor mole fraction of feed to tray j

F_V = molar feed rate of the V phase in a CSTR (mol/s)

h_V, h_L = heat transfer coefficients, for the film in V and L phase, respectively (W/m² K)

$H_{V,i}^0$ = vaporization enthalpy at the reference temperature (J/mol)

H_{VE}, H_{VI}, H_{VL}, H_{LE}, H_{LI}, H_{LL} = enthalpies: V phase entering, interface, and leaving; L phase entering, interface, and leaving, respectively (J/mol)

k = mass transfer coefficient (m/s)

K_i = distribution coefficient

l = film thickness (m)

L = liquid phase, completely mixed

m, n = parameters

n = number of components

N_t = total flux (mol/m² s)

N_V, N_L, N_{OV} = numbers of mass transfer units, V phase, L phase, and overall number for V phase, respectively

n_{VE}, n_{VL}, n_{LE}, n_{LL} = molar flows: V phase in, V phase out, L phase in, L phase out, respectively (mol/s)

p = system total pressure (Pa)

p_i^S = vapor pressure of pure component i (Pa)

P_V = molar product rate of the V phase in a CSTR (mol/s)

R = mass transfer resistance ratio

r = reaction (production of a component) (mol/m³ s)

Re = Reynolds number

Sc = Schmidt number

Sh = Sherwood number

T_V, T_{VE}, T_I, T_L, T^0 = temperatures: V phase outlet, V phase inlet, interface, and L phase; reference temperature for enthalpy (K)

V = vapor phase (plug flow)

V_j = total molar flow rate from tray j (mol/s)

V_m = molar volume (m³/mol)

V_R = volume of the reaction mixture in a CSTR (m³)

V_V = volume of the V phase (m³)

X_{CB} = relative conduction to boiling parameter

x_B, x_I, x_E, x_L = L phase mole fractions: in the bulk, at the interface, entering, and leaving, respectively

y^* = equilibrium mole fractions on V phase side

$y_{B,ave}$, y_I, y_E, y_L = V phase mole fractions: bulk average, at the interface, entering, and leaving, respectively

Greek letters

μ = viscosity (kg/ms)

γ = activity coefficient

λ = heat conductivity (W/mK)

ρ = density (kg/m³)

$[\beta]$ = bootstrap matrix

$[\Gamma]$ = thermodynamic correction matrix

$[\Xi]$ = high-flux correction matrix

$[\Psi]$ = mass transfer rate factor matrix

Ψ_{ave} = average mass transfer rate factor

δ_{ij} = Dirac delta function

Literature Cited

(1) Smith, L.; Taylor, R. Film Models for Multicomponent Mass Transfer: A Statistical Comparison. *Ind. Eng. Chem. Fundam.* **1983**, *22*, 97.

(2) Bird, R. B.; Stewart, W. E.; Lightfoot, E. N. *Transport Phenomena*; Wiley: New York, 1960.

(3) Taylor, R.; Krishna, R. *Multicomponent Mass Transfer*; Wiley: New York, 1993.

(4) Kooijman, H. A.; Taylor, R. Estimation of Diffusion Coefficients in Multicomponent Liquid Systems. *Ind. Eng. Chem. Res.* **1991**, *30*, 1217.

(5) Toor, H. L. Solution of the Linearized Equations of Multicomponent Mass Transfer: II. Matrix Methods. *AIChE J.* **1964**, *10*, 460.

(6) Taylor, R. Solution of the Linearized Equations of Multicomponent Mass Transfer. *Ind. Eng. Chem. Fundam.* **1982**, *21*, 407.

(7) McCabe, W. L.; Smith, J. C.; Harriot, P. *Unit Operations of Chemical Engineering*, 4th ed.; McGraw-Hill: New York, 1985.

(8) Alopaeus, V.; Nordén, H. V. Multicomponent Mass-Transfer Coefficient Correlation Generalizations. *Comput. Chem. Eng.* **1999**, *23*, 1177.

(9) Alopaeus, V.; Aittamaa, J.; Nordén, H. V. Approximate High Flux Corrections for Multicomponent Mass-Transfer Models and Some Explicit Methods. *Chem. Eng. Sci.* **1999**, *54*, 4267.

(10) Kooijman, H. A.; Taylor, R. Modelling Mass Transfer in Multicomponent Distillation. *Chem. Eng. J.* **1995**, *57*, 177.

(11) Reid, R. C.; Prausnitz, J. M.; Poling, B. E. *The Properties of Gases and Liquids*, 4th ed.; McGraw-Hill: New York, 1987.